Phase Conjugation and Negative Refraction using Nonlinear Active Metamaterials

Alexander R. Katko,[1] Shi Gu,[1] John P. Barrett,[1] Bogdan-Ioan Popa,[1] Gennady Shvets,[2] and Steven A. Cummer[1,*]

[1]*Department of Electrical and Computer Engineering and Center for Metamaterials and Integrated Plasmonics, Duke University, Durham, North Carolina 27708, USA*

[2]*Department of Physics, The University of Texas at Austin, Austin, Texas 78712, USA*

(Received 28 April 2010; published 17 September 2010)

We present an experimental demonstration of phase conjugation using nonlinear metamaterial elements. Active split-ring resonators loaded with varactor diodes are demonstrated theoretically to act as phase-conjugating or time-reversing discrete elements when parametrically pumped and illuminated with appropriate frequencies. The metamaterial elements were fabricated and shown experimentally to produce a time-reversed signal. Measurements confirm that a discrete array of phase-conjugating elements act as a negatively refracting time-reversal rf lens only 0.12λ thick.

DOI: 10.1103/PhysRevLett.105.123905 PACS numbers: 41.20.Jb, 42.65.Ky

Metamaterials are subwavelength structures which, when viewed macroscopically, achieve electromagnetic properties different from their constituent elements. This may include an effective negative refractive index [1], negative effective permeability [2], effective permittivity near zero [3], or many other unusual properties. Equally importantly, functionality can be embedded into metamaterials that can be difficult if not impossible to find in conventional materials. Examples of this approach include active metamaterials with [4–6] and without [7–9] gain for loss compensation and frequency tuning, respectively, as well as amplification [10]. Embedding a nonlinear response into metamaterials has also been used for power-dependent tuning [11–13] and coherent harmonic generation [14,15].

In this Letter we introduce a new class of nonlinear active metamaterials (NAMMs). Combining metamaterials' nonlinear response with an active high-frequency external excitation in the simplest metamaterial building block, the split-ring resonator (SRR), we experimentally demonstrate phase conjugation of microwave signals. Using numerical simulations, we demonstrate that such NAMM can be used as a building block for a negatively refracting lens. Negative refraction [16] is one of the most discussed and intriguing phenomena exhibited by a special class of metamaterials with negative permittivity and permeability. It was shown theoretically by Pendry [17], however, that negative refraction could also be produced by a thin slab of a material exhibiting time reversal (or, equivalently, phase conjugation). Traditional thick slabs of phase-conjugating (PC) media have been used for the useful property of generating negative frequency waves that focus back on the source, sometimes called retrodirectivity [18]. Discrete arrays of PC elements have also been used for retrodirectivity by the microwave community [19,20]. Pendry showed that a thin slab would indeed generate these retrodirective waves but would also generate a wave on the other side of the material exhibiting negative refraction. A few recent works have examined using discrete PC elements for forward focusing [21,22], but these cannot be extended to create an effective medium. As an example, [21] used an array of patch antennas for receiving; a phase-conjugating circuit for each antenna composed of PLLs, filters, phase shifters, IQ modulators, and other components; and a separate array of patch antennas for retransmission.

We demonstrate theoretically and experimentally that NAMMs, when driven with an active source, act as PC elements. The nonlinear characteristics of the metamaterials are obtained by embedding varactor diodes in each metamaterial element and exciting each element with a monochromatic rf signal, allowing easy extension to construction of a bulk medium of phase-conjugating SRRs with no external circuitry. We then demonstrate experimentally that nonlinear metamaterials do indeed act as phase-conjugating and thus negatively refracting elements, and in an array they act as a time-reversing material.

Parametric resonance can be used to realize phase conjugation in a single cell of a NAMM. Consider a single dipolelike nonlinear resonant scatterer with the parametrically modulated natural frequency $\Omega(t)$ given by $\Omega^2(t) = \Omega_0^2(1 + h_0 \sin(2\omega_0 t))$, where the $\Omega(t) = 1/\sqrt{L(t)C(t)}$ is related to the resonator's inductance L and capacitance C, one (or both) of which are modulated with the frequency $2\omega_0$ by the externally provided signal. The dimensionless parameter h_0 characterizes the strength of the parametric drive. Our experimental implementation relies on the modulation of the SRR's capacitance by inserting a nonlinear varactor whose capacitance depends on the externally applied high-frequency voltage. Further assume that SRRs are arrayed in the $z = 0$ plane along the y axis and subjected to an external monochromatic electromagnetic wave $E(y, t) = \sum_{k_y} E_{k_y} \exp[-i(\omega_1 t - k_y y)] + \text{c.c.}$ incident from the negative z direction and produced by a far-field source located at $z_{\text{source}} < 0$. The response of a single j's SRR, characterized by its induced dipole moment p_j, is calculated according to

$$\frac{d^2 p_j}{dt^2} + \gamma \frac{dp_j}{dt} + \Omega_0^2(1 + h_0 \sin(2\omega_0 t))p_j = \sum_{k_y} \Omega_0^2 E(k_y) a^3 e^{-i(\omega_1 t - k_y y_j)} + \text{c.c.}, \quad (1)$$

where y_j is the spatial location of the SRR-based NAMM, a is its effective size, and γ is the SRR's loss rate that includes dissipative and radiative losses. The effects of interelement interaction are assumed to be negligible owing to the tight field confinement. Equation (1) models a single SRR as a linear electric dipole with the low-frequency polarizability a^3 which is resonantly driven by the rf field of the antenna source. The solution of Eq. (1) can be expressed as $p_j = a_1^{(j)} \exp(-i\omega_1 t) + b_2^{(j)} \exp(i\omega_2 t)$, where $\omega_2 = 2\omega_0 - \omega_1$, and $a_1^{(j)}$, $b_2^{(j)}$ are computed by substituting p_j into Eq. (1) to obtain

$$a_1^{(j)} = \frac{\Omega^2 - \omega_2^2 + 2i\gamma\omega_2}{D(\omega_1)} e^{ik_y y_j}, \qquad b_2^{(j)} = \frac{ih_0\Omega^2}{2D(\omega_1)} e^{ik_y y_j}, \quad (2)$$

where the dispersion function $D(\omega_1)$ is given by

$$D = (\Omega^2 - \omega_1^2 - 2i\gamma\omega_1)(\Omega^2 - \omega_2^2 + 2i\gamma\omega_2) - h_0^2\Omega^4/4. \quad (3)$$

The electric field at $z > 0$ behind the plane of NAMMs is given by the sum of the incident fields and the fields produced by the induced dipole moments p_j of all NAMMs. Because the components of p_j proportional to a_1 have the same spatiotemporal dependence as the incident electric field $E(y, t)$, they produce scattered radiation which is spatially diverging away from the source. However, the contributions to p_j proportional to b_2 produce a phase-conjugated signal which, assuming that $\omega_2 \approx \omega_1$, produces a spatially converging field with the focus at $z_{\text{image}} = -z_{\text{source}} > 0$; i.e., the plane of NAMMs constitutes a flat negative-refraction lens.

The strongest phase-conjugated signal is produced when $\Omega_0 = \omega_0$ and $\omega_1 \approx \omega_0$. However, ω_2 can deviate from ω_1, significantly simplifying our experiments because the phase-conjugated signal has a different frequency from that of the incident field and is not overwhelmed by it. Note that, for certain values of ω_0, Ω_0, γ, and h_0, there exist complex solutions $\omega_* \equiv \omega_*^{(r)} + i\omega_*^{(i)}$ of $D(\omega_*) = 0$ corresponding to the parametric instability [23] with the growth rate $\omega_*^{(i)}$. For example, for $\omega = \Omega_0$ instability occurs if $h_0\omega_0 > 2\gamma_0$. For the rest of this Letter we assume that the strength of the parametric drive h_0 is small enough for the NAMM to remain stable.

Following the above analysis, we designed and fabricated SRR-varactor nonlinear metamaterial elements. They were designed to resonate near 950 MHz and have a pump signal delivered via cables directly to the varactors. Figure 1 shows the layout of an SRR with dimensions and corresponding photo of a fabricated SRR.

The SRRs were pumped with a signal at a specified pump frequency f_{pump} corresponding to $2\omega_0$. A monopole antenna located above a ground plane was used as the illumination source, radiating a signal at a specified source frequency f_{source} corresponding to ω_1. As described above, a nonlinearly generated, phase-conjugated signal should be reradiated at $f_{\text{pc}} = f_{\text{pump}} - f_{\text{source}}$ corresponding to ω_2.

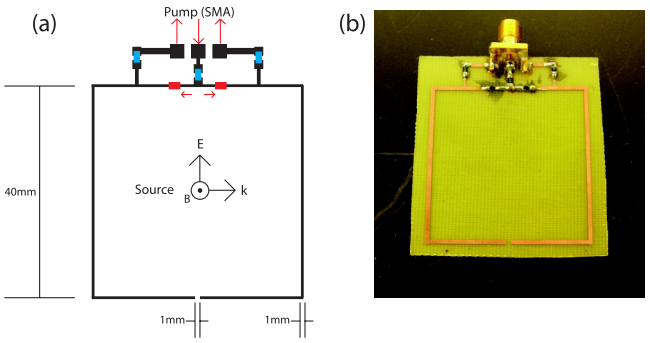

FIG. 1 (color online). (a) Layout of SRR element. Red (horizontal) elements are varactor diodes and blue (vertical) elements are isolation resistors. (b) Photo of fabricated SRR element.

Measurements were made using a spectrum analyzer with a receiving antenna to determine interference-free frequency bands and the frequencies were selected so that the mixed signal at f_{pc} was clearly distinct from the source signal at f_{source}. These experiments used frequencies of $f_{\text{pump}} = 1850$ MHz, $f_{\text{source}} = 950$ MHz, and subsequently $f_{\text{pc}} = 900$ MHz. Output from the spectrum analyzer is shown in Fig. 2 showing both the background signal levels and signal levels for the experiments with the pump and source signal generators switched on. As expected with our chosen frequencies, the signals at $f_{\text{pump}} = 1850$ MHz, $f_{\text{source}} = 950$ MHz, and $f_{\text{pc}} = 900$ MHz are only due to our experimental setup and not background radiation, demonstrating that the nonlinear SRRs are indeed generating a nonlinear mixed signal. The maximum measured value of the signal at f_{source} was -25.2 dBm. Through the experiments the maximum recorded value of the PC signal at f_{pc} was -49.6 dBm, yielding a minimum ratio of -24.4 dB between the source and PC signal. The source of this difference comes from the mixing efficiency in our experiments, which was not optimized in this work. Improving the coupling efficiency of the pump signal into the nonlinear metamaterial to overcome losses in the SRR will result in more efficient and practically relevant NAMMs. The signal at 925 MHz corresponds to the subharmonic of $\frac{f_{\text{pump}}}{2}$ and is present due to a power amplifier used in connection with the pump. The broad signal from approximately 868 to 888 MHz corresponds to the downlink band of GSM-850 cellular phone signals. This and the signal at 929 MHz are independent of our experiments but did not interfere at any frequencies. No higher order mixed frequency signals were detected and, along with the noted weak PC signal at least 24.4 dB down from the source, the assumptions in the analysis section are shown to be valid.

To verify that individual elements were PC, we measured the interference pattern generated by two isolated

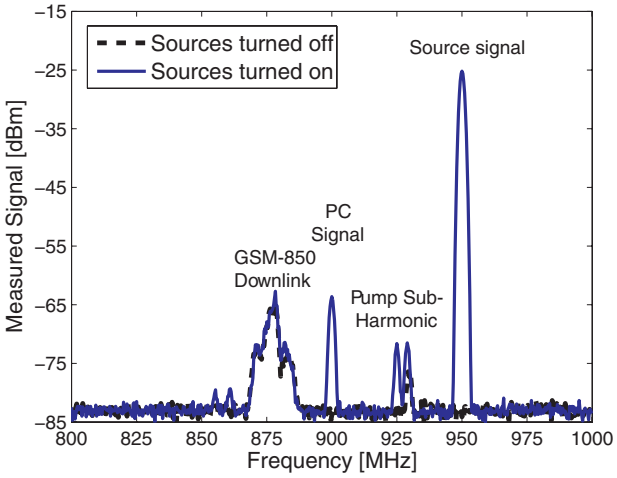

FIG. 2 (color online). Data from spectrum analyzer for background signal (dashed black) and pump and source signals switched on (solid blue). Notable frequencies include 900 MHz (f_{pc}), 950 MHz (f_{source}), and 1850 MHz (not shown).

elements. To map interference patterns, two monopole antennas above a ground plane were connected to a signal generator and spaced 1.5λ apart. A microwave absorber was placed between the antennas to isolate them. They were excited both in phase and $-90°$ out of phase, and the interference patterns were mapped at a constant distance λ from the line connecting the antennas, at the signal frequency, as illustrated in Fig. 3(b). For two normal, nonconjugating elements excited in phase and then $-90°$ out of phase, the maximum of the pattern moved to the right. Then the same interference patterns were measured at the mixed frequency with the SRRs in place. The absorber was used to ensure that only one antenna was illuminating each SRR. Again the antennas were excited in phase and then $-90°$ out of phase and the interference pattern was mapped at the mixed frequency. The measurements were interpolated and a filter was applied in the spatial Fourier domain to remove noise. The results are shown in Fig. 3(a) and a schematic is shown in Fig. 3(b).

Exciting two radiating elements with 0° phase shift and the same spatial positioning yielded field patterns roughly independent of the elements used, as shown by the solid lines in Fig. 3. The small-scale features in each curve are artifacts of a low dynamic range in these measurements. However, the important feature is the clear difference in the locations of the global extrema. Introducing a phase shift to the nonconjugating elements creates a maximum to the right of the center. However, with the NAMM elements, the peak moves to the opposite side of the center, showing that exciting normal radiating elements with a $-90°$ phase shift is equivalent to exciting the NAMM elements with a $+90°$ phase shift. This is a clear demonstration that the nonlinear SRRs act as phase-conjugating elements.

Three NAMM elements were then used to approximate a discrete slab of time-reversal medium. The thickness of the SRR array was approximately 0.12λ. The SRRs were

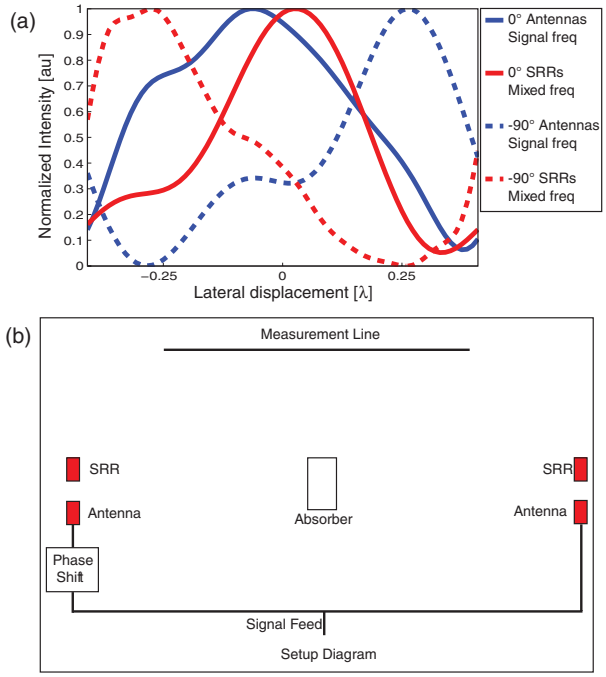

FIG. 3 (color online). (a) Interference pattern for in-phase antennas at f_{signal} (solid blue), $-90°$ out-of-phase antennas at f_{signal} (dashed blue), in-phase SRRs at f_{mixed} (solid red), $-90°$ out-of-phase SRRs at f_{mixed} (dashed red). (b) Schematic of setup (to scale). Antennas were fed at f_{signal} with both 0° and $-90°$ phase shifts. The absorber was used to isolate antennas and SRRs.

pumped in phase and illuminated with a single antenna. The SRRs were placed $\lambda/4$ apart, creating an array a total of $\lambda/2$ in width. The source antenna was placed a distance one λ normal to the array and $\lambda/2$ from the center of the array. The field power distribution of the mixed and phase-conjugated signal was then measured spatially to create a two-dimensional field map.

A simple calculation was used to generate the expected relative field distribution for phase-conjugating elements without considering details of the mixing efficiency of individual elements. The calculation assumed a r^{-1} dependence on the original signal, the generation of the nonlinear difference frequency in linear proportion to the incident signal, and a r^{-1} dependence and the measured radiation pattern of the SRRs for the reradiated signal. Its primary purpose was to predict the relative interference pattern for PC elements in a given geometry for comparison with measurements.

The field map was generated over a measurement area of dimensions $-3\lambda/2$ to $3\lambda/2$ tangential to the array and $\lambda/4$ to λ normal to the array again by using the spectrum analyzer. The raw data was interpolated and a filter was applied in the spatial Fourier domain to remove noise from the measurements. Figure 4 shows the results overlaid on the experimental setup.

The main beam at the phase-conjugated frequency f_{pc} clearly refracts to the opposite side of the normal compared

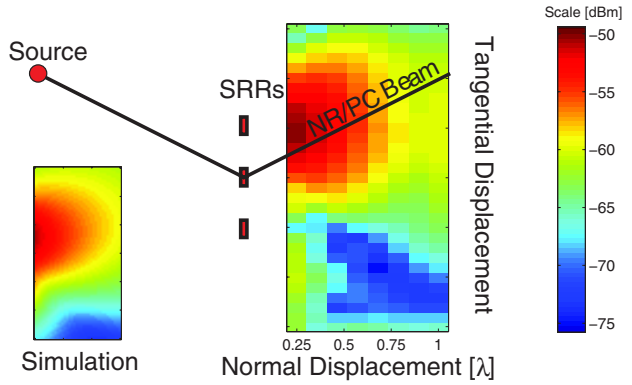

FIG. 4 (color online). Measured $abs(E)_{dBm}$ and experimental setup. The setup is approximately to scale. The source radiates from the upper left in the figure and SRRs produce a mixed signal at f_{pc}. The inset shows calculated results, exhibiting good agreement. The measurements show that the beam negatively refracts.

to a conventional material. Moreover, there is excellent agreement between measurement and calculation, as shown by the inset in the figure. The same calculation but assuming non-phase-conjugating elements was also conducted and yielded very different results. The field power along a line of constant distance from the array was examined to illustrate this more quantitatively, comparing conjugate calculation, nonconjugate calculation, and filtered measured data. This is presented in Fig. 5.

An array of PC metamaterials is limited in far-field imaging ability only by normal imaging considerations like aperture size and spacing between elements. Creating a larger array with more PC elements provides a better approximation of an infinite, continuous medium and thus provides a closer approximation to an ideal far-field lens. We have shown that NAMMs can be used to create a simple and effective phase-conjugating medium and provided a path towards realizing time-reversal metamaterial media.

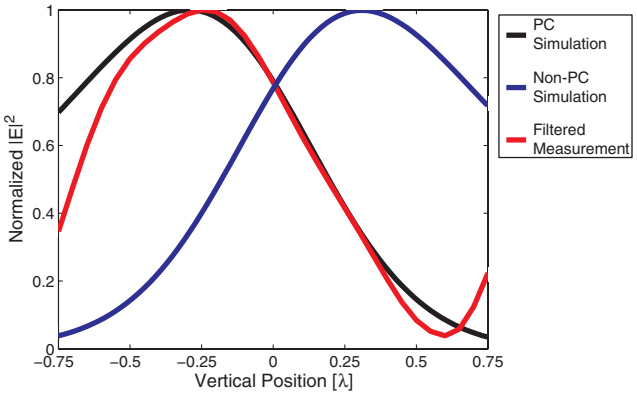

FIG. 5 (color online). Normalized intensity at constant distance from array for various data sets: calculated data for phase-conjugating elements (black); calculated data for non-phase-conjugating elements [dark gray (blue)]; and filtered measured data [light gray (red)]. The measured data match calculated data very well and are negatively refracted when compared to non-PC simulated data.

In summary, we first demonstrated theoretically that metamaterials with embedded nonlinear elements produce a phase-conjugated or time-reversed signal through parametric pumping. Two element experiments unambiguously demonstrated the phase conjugation of the mixed signal, and measurements of the field distribution produced by a 3 element array showed the expected effective negative-refraction behavior of the time-reversed signal. Such elements form a simple but powerful building block for more complex phase-conjugation media and devices, and we have shown that this class of active nonlinear metamaterials is promising for realizing designs utilizing time-reversal media and thin-slab rf imaging.

This work was supported in part by DARPA under Contract No. HR0011-05-C-0068. G. S. would like to acknowledge the support of the U.S. Air Force Office of Scientific Research (AFOSR) MURI Grants No. FA 9550-06-1-0279 and No. FA 9550-08-1-0394.

*cummer@ee.duke.edu

[1] D. R. Smith *et al.*, Phys. Rev. Lett. **84**, 4184 (2000).
[2] J. Pendry *et al.*, IEEE Trans. Microwave Theory Tech. **47**, 2075 (1999).
[3] R. W. Ziolkowski, Phys. Rev. E **70**, 046608 (2004).
[4] Y. Yuan, B.-I. Popa, and S. Cummer, Opt. Express **17**, 16 135 (2009).
[5] B.-I. Popa and S. Cummer, Microw. Opt. Technol. Lett. **49**, 2574 (2007).
[6] A. Fang *et al.*, Phys. Rev. B **79**, 241104(R) (2009).
[7] H.-T. Chen *et al.*, Nature (London) **444**, 597 (2006).
[8] O. Reynet and O. Acher, Appl. Phys. Lett. **84**, 1198 (2004).
[9] D. Wang *et al.*, Appl. Phys. Lett. **91**, 164101 (2007).
[10] R. Syms, L. Solymar, and I. Young, Metamaterials **2**, 122 (2008).
[11] B. Wang *et al.*, Opt. Express **16**, 16 058 (2008).
[12] D. Huang, E. Poutrina, and D. Smith, Appl. Phys. Lett. **96**, 104104 (2010).
[13] I. Shadrivov, S. Morrison, and Y. Kivshar, Opt. Express **14**, 9344 (2006).
[14] Z. Wang *et al.*, Appl. Phys. Lett. **94**, 134102 (2009).
[15] M. W. Klein *et al.*, Science **313**, 502 (2006).
[16] V. Veselago, Sov. Phys. Usp. **10**, 509 (1968).
[17] J. B. Pendry, Science **322**, 71 (2008).
[18] A. Yariv, IEEE J. Quantum Electron. **14**, 650 (1978).
[19] L. Chiu *et al.*, Microw. Opt. Technol. Lett. **48**, 409 (2006).
[20] C. Pon, IEEE Trans. Antennas Propag. **12**, 176 (1964).
[21] V. F. Fusco, N. B. Buchanan, and O. Malyuskin, IEEE Trans. Antennas Propag. **58**, 798 (2010).
[22] O. Malyuskin and V. Fusco, IEEE Trans. Antennas Propag. **58**, 459 (2010).
[23] L. D. Landau and E. M. Lifshitz, *Mechanics* (Pergamon Press, New York, 1976), 3rd ed.